



LAWRENCE  
LIVERMORE  
NATIONAL  
LABORATORY

# Solid-state Rayleigh-Taylor experiments in vanadium at Mbar pressures at the Omega laser

B. A. Remington, H. S. Park, K. T. Lorenz, R. M.  
Cavallo, S. M. Pollaine, S. T. Prisbrey, R. E. Rudd, R.  
C. Becker, J. V. Bernier

August 27, 2009

Joint U.S.-Russia Conference on Advances in Materials  
Science

Prague, Czech Republic

August 31, 2009 through September 3, 2009

## **Disclaimer**

---

This document was prepared as an account of work sponsored by an agency of the United States government. Neither the United States government nor Lawrence Livermore National Security, LLC, nor any of their employees makes any warranty, expressed or implied, or assumes any legal liability or responsibility for the accuracy, completeness, or usefulness of any information, apparatus, product, or process disclosed, or represents that its use would not infringe privately owned rights. Reference herein to any specific commercial product, process, or service by trade name, trademark, manufacturer, or otherwise does not necessarily constitute or imply its endorsement, recommendation, or favoring by the United States government or Lawrence Livermore National Security, LLC. The views and opinions of authors expressed herein do not necessarily state or reflect those of the United States government or Lawrence Livermore National Security, LLC, and shall not be used for advertising or product endorsement purposes.

## **Solid-state Rayleigh-Taylor experiments in vanadium at Mbar pressures at the Omega laser**

**B. A. Remington,<sup>1</sup> H.S. Park, K. T. Lorenz, R. M. Cavallo, S. M.  
Pollaine, S. T. Prisbrey, R. E. Rudd, R. C. Becker, and J. V. Bernier**

Lawrence Livermore National Laboratory, Livermore, CA 94550 USA

*We present experiments on the Rayleigh-Taylor (RT) instability in the plastic flow regime of solid-state vanadium (V) foils at ~1 Mbar pressures and strain rates of  $10^6$ - $10^8$  s<sup>-1</sup>, using a laser based, ramped-pressure acceleration technique. High pressure material strength causes strong stabilization of the RT instability at short wavelengths. Comparisons with 2D simulations utilizing models of high pressure strength show that the V strength increases by a factor of 3.5 at peak pressure, compared to its ambient strength. An effective lattice viscosity of ~400 poise would have a similar effect.*

### **Introduction**

The Rayleigh-Taylor (RT) instability in the presence of solid state, material strength is of considerable interest. High explosive (HE) driven experiments to study RT instability growth in solid state aluminum at peak pressures and strain rates of  $P_{\text{max}} \sim 100$  kbar and  $\dot{\epsilon} \sim 10^5$  s<sup>-1</sup> were developed in the 1970s, and showed strong RT stabilization of short-wavelength perturbations. [1] More recently, HE-driven RT experiments have been done in several different metals (Al, Cu, V) at 300-700 kbar peak pressures in planar geometry, and at pressures reaching ~3 Mbar in convergent cylindrical geometry. [2] Using a newly developed, laser based, ramped pressure drive, experiments have been performed at  $P_{\text{max}} \sim 200$  kbar and  $\dot{\epsilon} \sim 10^6$  s<sup>-1</sup> in Al. [3] We report here results from an RT experiment using a laser generated ramped pressure drive, reaching  $P_{\text{max}} \sim 1$  Mbar pressures at strain rates of  $10^6$ - $10^8$  s<sup>-1</sup> in solid-state vanadium (V), a ductile body-centered cubic (BCC) metal. Strong RT stabilization is observed. [4]

### **Method**

We use six azimuthally symmetric laser beams at the Omega Laser, [5] each with  $E_L \sim 135$  J energy at laser wavelength of  $\lambda_L = 351$  nm and 3.7 ns square pulse shape, to generate our drive. The ~640  $\mu\text{m}$  diameter flat-top spatial profile is achieved using continuous phase plates (CPP) on the drive beams, creating an average peak laser intensity of  $I_L \sim 2.5 \times 10^{13}$  W/cm<sup>2</sup>. This launches a strong shock into a reservoir consisting of 40  $\mu\text{m}$ -thick polyimide, 125  $\mu\text{m}$  thick polycarbonate, and 35  $\mu\text{m}$  thick 2% brominated polystyrene,  $\text{C}_{50}\text{H}_{48}\text{Br}_2$ , all glued together. The CH(Br) layer absorbs low energy x-rays generated at the ablation front. When the shock breaks out the back of the reservoir, the plasma releases (unloads) across the 300  $\mu\text{m}$  vacuum gap and stagnates on the V sample, creating a ~1 Mbar ramped pressure drive. [6,7] This causes the 35  $\mu\text{m}$

---

<sup>1</sup> remington2@llnl.gov

thick V sample to accelerate at a peak value of  $g \sim 5 \times 10^{13} \text{ cm/s}^2$ . In order to insulate the rippled vanadium sample from the heat created by the initial stagnating plasma, we use a 6  $\mu\text{m}$  thick, CH-based epoxy layer, conformal on the ripple side and machined flat on the gap side, as a heat shield. The accelerating rippled sample is RT unstable, and the ripple amplitude increases at a rate that is reduced due to material strength.

We measure the drive using a line VISAR velocity diagnostic [8] on separate targets consisting of a 10  $\mu\text{m}$  thick Al foils backed by a LiF window for a range of laser energies. A streaked VISAR image from one of the drive shots is shown in the inset of Fig. 1. We then use the radiation-hydrodynamics code LASNEX [9] to determine the plasma drive, which is a set of material density, velocity, and temperature profiles as a function of position from the unloading reservoir just prior to impacting the sample. The plasma drive applied to the V sample generates a ramped loading reaching  $P_{\text{max}} \sim 900$  kbar, as shown in Fig. 1, and compressions of  $\rho/\rho_0 \sim 1.3$ -1.4. Figure 2 shows the corresponding equivalent plastic strain versus time in the V sample, from a 1D radiation-hydrodynamics simulation. The V sample is predicted to stay factors of 3-5 below the melt temperature, as shown in the inset in Fig. 2. The 35  $\mu\text{m}$  thick V sample was made with a  $\lambda = 60 \mu\text{m}$  wavelength,  $\eta_0 = 0.6 \mu\text{m}$  amplitude sinusoidal ripple on its surface by a sputtering technique. [10] The vanadium samples were full density, had an average grain size of  $\sim 1 \mu\text{m}$  in the lateral direction, 3-5  $\mu\text{m}$  in the thickness (columnar) direction, and a measured tensile strength at ambient pressure and low strain rate of 715 MPa [10].

## Results and Discussion

To measure the RT ripple growth, we used face-on radiography with a 5.2 keV laser driven vanadium He- $\alpha$  x-ray backlighter, either in an area backlighting or a point projection imaging configuration. The area backlighting technique uses a large area x-ray source and a gated x-ray camera with 15  $\mu\text{m}$  pinholes run at magnification of  $\sim 6$ . [3] The point projection technique uses a  $\sim 15 \mu\text{m}$  diameter pinhole aperture just in front of the V backlighter foil to create point projection imaging at magnification  $\sim 19$ , onto a gated x-ray camera. The inset in Fig. 3 shows an example of a radiographic image of ripple growth at a delay time of 80 ns relative to the start of the drive laser. The RT-induced perturbation growth is written as a growth factor,  $\text{GF}(t) = \Delta\text{OD}(t)/(\Delta\text{OD}_0 \cdot \text{MTF})$ , where  $\Delta\text{OD}(t)$  is the optical depth modulation due to the ripple at time  $t$ ,  $\Delta\text{OD}_0 = \eta_0/\lambda_{\text{mfp}}$  is the initial optical depth,  $\lambda_{\text{mfp}} \sim 19.6 \mu\text{m}$  is the mean free path length of the 5.2 keV backlighter x rays in vanadium, and MTF is the modulation transfer function, which quantifies the diagnostic spatial resolution. The  $\Delta\text{OD}(t)$  is measured from the radiograph by Fourier analysis of the ripple lineouts. The self-consistent data set spanning several shot campaigns is shown by the red plotting symbols in Fig 3. Typical errors in the measured growth factors were  $\delta\text{GF}/\text{GF} \sim 10\%$  or less. We estimate an average strain rate,  $\dot{\epsilon}_{\text{av}} \sim 3 \times 10^7 \text{ s}^{-1}$ , by fitting a linear slope to the simulated strain vs. time (see Fig. 2) over the interval of 25-40 ns. For  $t > 40$  ns, this drops to  $\dot{\epsilon}_{\text{av}} \sim 3 \times 10^6 \text{ s}^{-1}$ .

We compare our ripple growth data to an analytic RT model that treats strength as an effective lattice viscosity. In the linear regime, classical RT growth can be written as  $\text{GF} \approx e^{\int \gamma_{\text{classical}} dt}$ , where  $\gamma_{\text{classical}} \approx [A \cdot \frac{2\pi}{\lambda} \cdot g(t)]^{1/2}$  gives the growth rate for inviscid fluids, and  $A$ ,  $\lambda$ , and  $g$  are the Atwood number, perturbation wavelength, and foil acceleration,

respectively. For viscous fluids, the RT growth rate is expressed in the dispersion relation,  $\gamma_{RT}^2 + 2k^2\nu\gamma_{RT} - gkA = 0$ , [12,13], where  $\nu(\text{cm}^2/\text{s}) = \mu/\rho$  is the kinematic viscosity,  $\mu(\text{dyne}\cdot\text{sec}/\text{cm}^2 = \text{poise})$  is the dynamic viscosity, and  $\rho$  is density. We show these analytic results in Fig. 3 for RT growth factors versus time. The analytic classical inviscid RT calculation for no strength is shown by the top curve, followed by the viscous model for (in order from the top) dynamic viscosities of 100, 200, 400, and 800 poise. The best fit viscosity was  $\sim 400$  poise under these conditions. As a consistency check, we use a relationship equating strength with an effective lattice viscosity,  $\nu = \mu/\rho \approx \sigma/(\sqrt{6}\rho\langle\dot{\epsilon}\rangle)$ , [12] giving  $\sigma \approx \sqrt{6}\langle\dot{\epsilon}\rangle\mu$ . Using the average strain rate of  $\langle\dot{\epsilon}\rangle \approx 3 \times 10^7 \text{ s}^{-1}$  over the interval of 25-40 ns from the 1D simulations (see Fig. 2) and the fitted viscosity of 400 poise gives an estimated peak strength of 29 kbar. A rough approximation of strain rate can also be made from  $\langle\dot{\epsilon}\rangle \approx \frac{1}{3}\dot{\rho}/\rho \approx \frac{1}{3}(\Delta\rho/\rho_0)/\Delta t_{\text{rise,time}}$ . [6] From the equation of state of V, an estimated compression of  $\rho/\rho_0 \sim 1.4$  occurs over the measured rise time of  $\sim 6$  ns, giving  $\langle\dot{\epsilon}\rangle \approx 2 \times 10^7 \text{ s}^{-1}$ , and hence, a rough peak strength estimate of 19 kbar.

The PTW model is a strain rate dependent strength model, based on deformation by thermal activation for low strain rates and viscous phonon drag for high strain rates. [13] The dimensionless shear strength in the low-strain limit is expressed as:

$$\hat{\tau}_y = \max\left\{y_0 - (y_0 - y_\infty)\text{erf}[\kappa\hat{T}\ln(\gamma\dot{\xi}/\dot{\epsilon})], s_0(\dot{\epsilon}/\gamma\dot{\xi})^\beta\right\}, \quad (1)$$

where  $\dot{\epsilon}$  is the strain rate,  $\hat{T}$  is the normalized temperature,  $T_{\text{melt}} = T_{\text{melt}}(\rho)$  is the calculated melt temperature based on the Lindeman model, [14]  $\dot{\xi}$  is a reference inverse time scale,  $\gamma\dot{\xi} = \dot{\epsilon}_{\text{crit}}$  is the critical strain rate above which the deformation switches from thermal activation to phonon drag, and  $y_0, y_\infty, \kappa, \gamma, s_0$ , and  $\beta$  are material dependent input parameters. The dimensionless shear strength,  $\hat{\tau}_s$ , in the (saturated) high-strain limit has a similar form, only with  $s_0$  and  $s_\infty$  replacing  $y_0$  and  $y_\infty$ . These are combined in a Voce work hardening prescription to give the predicted (dimensional) material strength. To fit our experimental data with 2D simulations using the PTW model, we lowered the critical strain rate for the transition from thermal activation to the phonon drag regime from the default value of  $\gamma\dot{\xi} \sim 10^9 \text{ s}^{-1}$  to  $\sim 10^6 \text{ s}^{-1}$ . This was accomplished by multiplying the PTW input parameters  $\gamma, y_0$ , and  $s_0$  by 1/800, 0.60, and 0.69, respectively, as illustrated in Fig. 4. [15] These changes to the PTW input parameters leave the strength predictions at  $\dot{\epsilon} < 10^6 \text{ s}^{-1}$  (thermal activation regime) unchanged, while increasing the strength for  $\dot{\epsilon} > 10^6 \text{ s}^{-1}$  (phonon drag regime). The default PTW parameters for V in the high- $\dot{\epsilon}$  regime were set by overdriven shock experiments in Ta, also a BCC metal. [13] So it is not surprising that substantial changes in these input parameters for ramp loaded V were required.

The 2D simulation results using this modified PTW strength model essentially goes right through the experimental data (not shown). The calculated average peak flow stress (strength) is  $\sim 25$  kbar based on these 2D simulations, corresponding to a peak pressure and strain rate of 900 kbar and  $3 \times 10^7 \text{ s}^{-1}$ . This is a factor of 3.5 higher than the measured ambient strength of 7.15 kbar, [11]. We estimate the uncertainties in inferred

strength from uncertainties in (1) the experimental growth factor measurements and (2) our drive model to each be ~15%. Assuming that these are independent sources of error, this gives an overall estimated uncertainty in inferred peak strength of ~20%.

## **Conclusions**

Our experiments show that (solid-state) vanadium strength is very effective at stabilizing RT instability growth at ~Mbar pressures and very high ( $10^6$ - $10^8$  s<sup>-1</sup>) strain rates. The deformation mechanism is suggested to be viscous phonon drag. A peak strength of vanadium at  $P_{\text{max}} \sim 900$  kbar and  $3 \times 10^7$  s<sup>-1</sup> was estimated to be ~25 kbar, which is a factor of 3.5 higher than the ambient strength, with an estimated uncertainty of ~20%. Analytic estimates show that an effective lattice viscosity of ~400 poise would have a similar stabilizing effect. Designs to extend these experiments to pressures  $P \gg 1$  Mbar on NIF [16] have been developed. [17]

## **Acknowledgements**

- This work was performed under the auspices of the U.S. Department of Energy by Lawrence Livermore National Laboratory under Contract No. DE-AC52-07NA27344.

## **References**

- [1] J. F. Barnes et al., J. Appl. Phys. 45, 727 (1974); *ibid*, 51, 4678 (1980).
- [2] A.I. Lebedev et al., in Shock Compression of Condensed Matter – 2005, edited by M.D. Furnish, M. Elert, T.P. Russell, and C.T. White (AIP, 2006), p. 745.
- [3] K.T. Lorenz et al. Phys. Plasmas 12 (2005), 056309.
- [4] H.S. Park et al., submitted, Phys. Rev. Lett. (2009).
- [5] T.R. Boehly et al., Opt. Commun. 133, 495 (1997).
- [6] J. Edwards et al., Phys. Rev. Lett. 92 (2004), 075002.
- [7] K.T. Lorenz et al. HEDP 2 (2006), 113.
- [8] P.M. Celliers et al., Appl. Phys. Lett. 73, 1320 (1998).
- [9] G.B. Zimmerman, W.L. Kruer, Com. Plasma Phys. Control. Fusion 2, 51 (1975).
- [10] A.F. Jankowski, J. Go, J.P. Hayes, Surface & Coatings Tech. 202 (2007), 957.
- [11] K.O. Mikaelian, Phys. Rev. E 47, 375 (1993).
- [12] J.D. Colvin et al., J. Appl. Phys. 93, 5287 (2003).
- [13] D.L. Preston, D.L. Tonks, and D.C. Wallace, J. Appl. Phys. 93, 211 (2003).
- [14] D.J. Steinberg, S.G. Cochran, and M.W. Guinan, J. Appl. Phys. 51, 1498 (1980).
- [15] B.A. Remington et al., Mat. Sci. Tech. 22, 474 (2006).
- [16] C.A. Haynam et al., Appl. Optics 46, 3276 (2007).
- [17] H. S. Park et al., J. Phys.: Conf. Ser. 112, 042024 (2008).

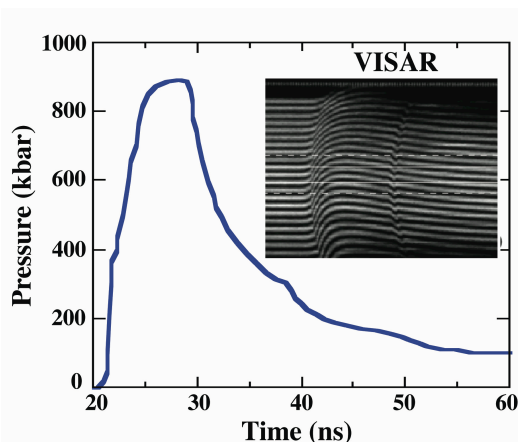


Figure 1

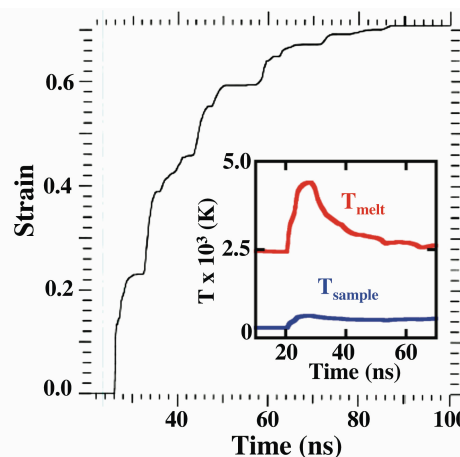


Figure 2

Fig. 1. Pressure vs. time in the vanadium RT sample, as calculated from 1D radiation-hydrodynamics simulations, adjusted to reproduce the drive measured in the Al-LiF witness plates. The inset shows a raw line VISAR image for the Al-LiF drive shot.

Fig. 2. The simulation of plastic strain vs. time in the V sample, from a 1D radiation-hydrodynamics simulation. The inset shows the melt temperature (from the Lindemann melt law) and sample temperature, both from the radiation-hydrodynamics simulations.

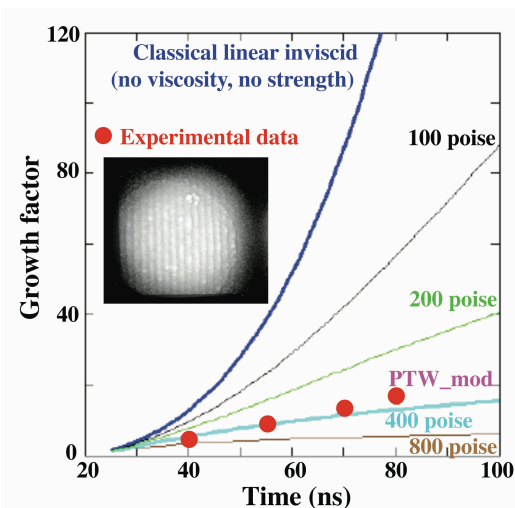


Figure 1

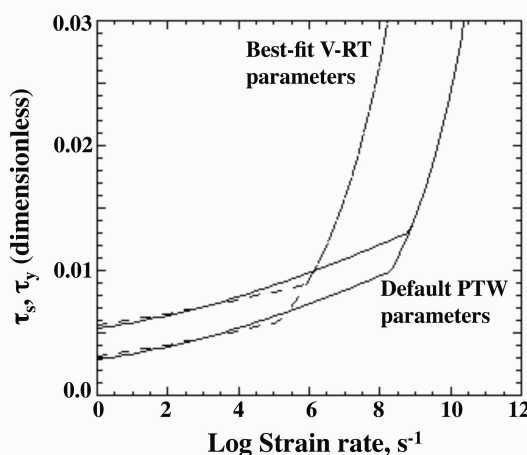


Figure 2

Fig. 3. Calculated perturbation growth factor vs. time from an analytic RT theory in a viscous medium corresponding to dynamic viscosities of (from the top) 0, 100, 200, 400, and 800 poise. The experimental data is given by the solid red circle plotting symbols; a raw experimental 2D x-ray radiograph at 80 ns is given in the inset.

Fig. 4. Dimensionless strength vs log(strain rate) for the PTW model using default input parameters for V (solid curves), and modified PTW input parameters to fit the experimental data (dashed curves). The upper curves are for work-hardened saturated strength,  $\tau_s$ , and the lower curves correspond to the small strain limit,  $\tau_y$ .